

Single-particle and transport scattering times in a back-gated GaAs/Al_xGa_{1-x}As modulation-doped heterostructure

B. Das and S. Subramaniam

Department of Electrical Engineering, University of Notre Dame, Notre Dame, Indiana 46556

M. R. Melloch and D. C. Miller*

School of Electrical Engineering, Purdue University, West Lafayette, Indiana 47907

(Received 12 November 1992)

The transport and single-particle scattering times characterizing a two-dimensional electron gas in a back-gated GaAs/Al_xGa_{1-x}As modulation-doped heterostructure are investigated as a function of the carrier density. For a factor-of-3 change in the carrier density, the ratio of transport scattering time to single-particle relaxation time is observed to vary from 2 to 10. The data agree with theoretical model(s) only if multiple small-angle scattering events are assumed to be correlated.

I. INTRODUCTION

Electron transport in semiconductors is generally characterized by a transport scattering time, τ_t , that is defined by the relaxation-time approach to the Boltzmann equation, and is related to the dc conductivity, σ , through $\sigma = n_s e^2 \tau_t / m^*$. However, there is also a single-particle scattering time, τ_s , which characterizes the quantum-mechanical broadening Γ of single-particle electron states, defined as $\tau_s = \hbar / 2\Gamma$. The single-particle scattering time is an important parameter in many theoretical calculations, since it is a measure of the effect of the electron-impurity interaction on the density of states. The decay time for such single-particle excitations (also called quantum lifetime) is given by

$$\frac{1}{\tau_s} = \int_0^\pi Q(\theta) d\theta, \quad (1)$$

where $Q(\theta)$ is proportional to the scattering through an angle θ . On the other hand, the transport scattering time is given by

$$\frac{1}{\tau_t} = \int_0^\pi Q(\theta)(1 - \cos\theta) d\theta. \quad (2)$$

Since all scattering events contribute with equal weight to τ_s , while τ_t is not sensitive to small-angle scattering, the two times, in general, are not identical. For short-range scattering potentials, like interface-roughness scattering in metal-oxide-semiconductor (MOS) structures, the two scattering times are the same.¹ However, in modulation-doped heterostructures, where the dominant scattering mechanism is the long-range potential arising from remote ionized impurities, the two scattering times τ_t and τ_s can differ significantly. The ratio of the two times τ_t/τ_s is expected to vary with carrier density. In this paper, we report the results of our investigations of the dependence of this ratio on the two-dimensional electron-gas (2DEG) carrier density in a back-gated GaAs/Al_xGa_{1-x}As modulation-doped heterostructure. The 2DEG density in our structure can be varied by applying a voltage between a frontside Ohmic contact and

the conducting substrate which acts as a back-gate. Changing n_s in this way does not affect the density or the configuration of the remote ionized impurities.

The ratio τ_t/τ_s for a 2DEG has been investigated theoretically and experimentally by a number of researchers. Das Sarma and Stern¹ have calculated τ_t and τ_s due to remote ionized impurity scattering and predicted their dependence on spacer layer thickness as well as the carrier density. Gold² has investigated the effects of interface-roughness scattering, alloy scattering, and remote ionized impurity scattering on the scattering times in the GaAs and In_xGa_{1-x}As material systems. It is believed that in GaAs/Al_xGa_{1-x}As modulation-doped heterostructures, at low temperatures, remote ionized impurity scattering is the dominant scattering mechanism. Also, for remote ionized impurity scattering,² $\tau_t/\tau_s = 1$ for $2k_F\alpha \ll 1$ and $\tau_t/\tau_s = (2k_F\alpha)^2$ for $2k_F\alpha \gg 1$, where α is the spacer layer width and k_F is the Fermi wave vector. In other words, for low carrier densities, the ratio of τ_t/τ_s is unity, while for higher densities, the ratio varies linearly with the carrier density.

Experimentally, the ratio of transport and single-particle scattering times has been investigated by Coleridge³ for samples with a range of carrier concentrations obtained by changing the spacer layer thickness. The experimental data were obtained from a number of samples grown over a period of four years, during which time the background impurity concentration also changed. It was recognized by Coleridge that the background impurity concentration affects the scattering times. The ratio of scattering times obtained experimentally was much smaller than the theoretical predictions. However, Coleridge showed that if the theoretical calculations were modified to assume that multiple small-angle-scattering events are correlated, then there was good agreement with experimental data. That multiple small-angle-scattering events from remote ionized donors are correlated has also been pointed out by other authors.⁴⁻⁶ Investigations by Fang, Smith III, and Wright⁷ on GaAs/Al_xGa_{1-x}As modulation-doped heterostructures with spacer layer thicknesses varying from 1.5 to 50

nm showed excellent agreement with the calculations of Das Sarma and Stern. For a 200-Å spacer layer, the ratio τ_t/τ_s was 34.5, which is significantly higher than typical values reported. As pointed out by Coleridge,³ such large numbers were obtained due to the fact that the τ_s in Ref. 7 was calculated from the Shubnikov-de Haas (SdH) amplitude multiplied by an extra factor of H^2 . The variation of τ_t/τ_s with spacer layer thickness and doping density was also investigated by Bockelmann *et al.*⁸ The experimental data on τ_s were not conclusive, but τ_t decreased with increasing n_s . Harrang *et al.*⁹ investigated the variation of τ_t/τ_s with a top-gate voltage but did not observe any clear variations with the gate voltage. Also, no correlation with carrier density was attempted. The variation of τ_t/τ_s with carrier density was investigated by Mani and Anderson¹⁰ where the carrier density was varied by illuminating the sample and thus using the persistent-photoconductivity (PPC) effect. The data showed a decrease in τ_t/τ_s with increased carrier density, which contradicts the theoretical predictions.^{1,2} The explanation proposed was that the deep centers that are responsible for the PPC effect might be the dominant factor in limiting the single-particle scattering time.

II. EXPERIMENTAL PROCEDURE AND RESULTS

A schematic cross section of the GaAs/Al_xGa_{1-x}As wafer used in this experiment is shown in Fig. 1. The sample was grown by molecular-beam epitaxy (MBE) on a p^+ conducting substrate. The sample is modulation doped consisting of a 600-Å n^+ -Al_xGa_{1-x}As layer (doped $\sim 10^{18} \text{ cm}^{-3}$) separated from the 2DEG by a 200-Å undoped Al_xGa_{1-x}As spacer layer. The 1- μm -thick undoped i -GaAs layer (background doping of 10^{14} – 10^{15} cm^{-3}) acts as an insulating layer at liquid-helium temperatures and allows the application of a back-gate voltage with low leakage currents.

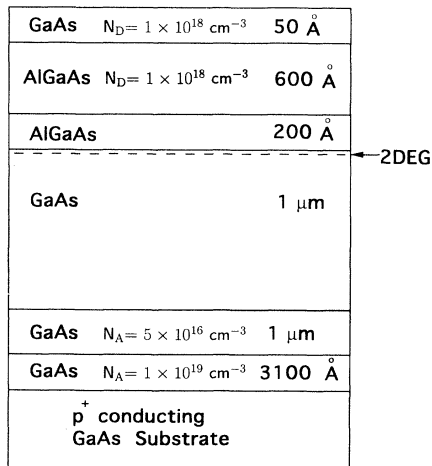


FIG. 1. Schematic cross section of the experimental structure. The 2- μm i -GaAs layer (insulating at low temperatures) allows carrier densities to be varied by back-gating with low leakage currents.

A number of Hall bars were fabricated using standard photolithography, Ohmic contact metallization, lift off, and Ohmic contact annealing. It may be noted that the 2DEG in this structure lies at a depth of 850 Å below the surface and that the p^+ conducting substrate is 2 μm below the 2DEG. This requires that the Ohmic contacts diffuse at least 850 Å down to the 2DEG, but do not diffuse deep enough to give rise to large leakage currents. To achieve this, a systematic study of the dependence of leakage currents on process parameters was performed and is reported elsewhere.¹¹

SdH and low-field Hall measurements were performed in a pumped liquid-helium cryostat at a temperature of 1.4 K using an iron core magnet capable of producing a magnetic field up to 1 T. The samples were cooled in the dark to avoid the PPC effect.

The carrier density of the sample was varied by applying a voltage between the conducting substrate (back-gate) and a front-side Ohmic contact, ranging from -5 to $+0.5$ V. Over this range the leakage current was less than 5 nA. SdH and Hall measurements were performed at different fixed back-gate voltages. The excitation current used for the measurements was kept low to avoid electron heating. The SdH data indicate that there is only one subband populated in this sample, since a single frequency is observed. The carrier densities obtained from Hall and SdH measurements agree within 3%. The transport mobility at each back-gate voltage was calculated from the zero magnetic field resistivity and the carrier density. Figure 2 shows the variation of the carrier density and the concomitant variation of the transport mobility as a function of the back-gate voltage. It can be seen that the carrier density varies linearly with the back-gate voltage and changes by more than a factor of 3 in the range of voltage applied. The mobility varies with gate voltage and hence with carrier density as $\mu \sim n_s^\gamma$, where $\gamma = 2.0$. The observed value of the exponent γ is greater than that predicted theoretically for remote ionized impurity scattering ($\gamma \sim 1.5$), but such a discrepancy has been observed before¹² for high-mobility samples. Figure 3 shows SdH data measured with various back-

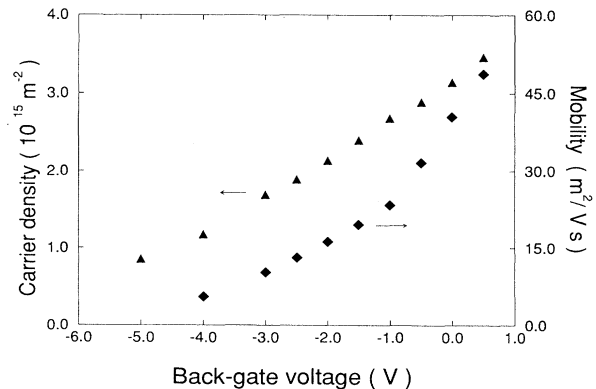


FIG. 2. The variation of the carrier density and the transport mobility with back-gate voltage.

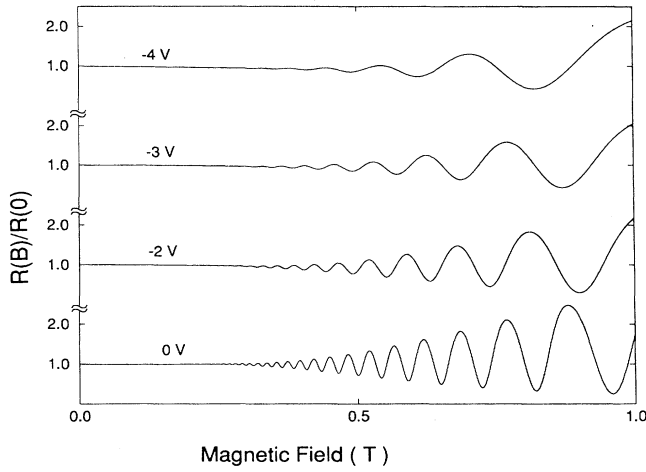


FIG. 3. Shubnikov-de Haas oscillations at different back-gate voltages. The resistances are normalized and the curves are shifted for clarity. However, no background has been subtracted. The lack of a positive or negative background magnetoresistance allows precise measurement of the single-particle scattering times from Dingle plots, as shown in Fig. 4.

gate voltages applied. It is clear from the figure that with more negative voltages, both the frequency of the SdH oscillations (proportional to n_s) and the amplitude of the SdH oscillations (related to τ_s) decrease.

The single-particle scattering time is related to the amplitude of the SdH oscillations and was calculated from Dingle plots.³ The expressions given by Ando¹³ and Ishihara and Smrčka¹⁴ for the magnetoconductivity, valid for low fields, do not distinguish between long-range scattering and short-range scattering. Coleridge, Stoner, and Fletcher¹⁵ offered a modified expression which made a distinction between the momentum relaxation time and the single-particle scattering time. The amplitude ΔR of

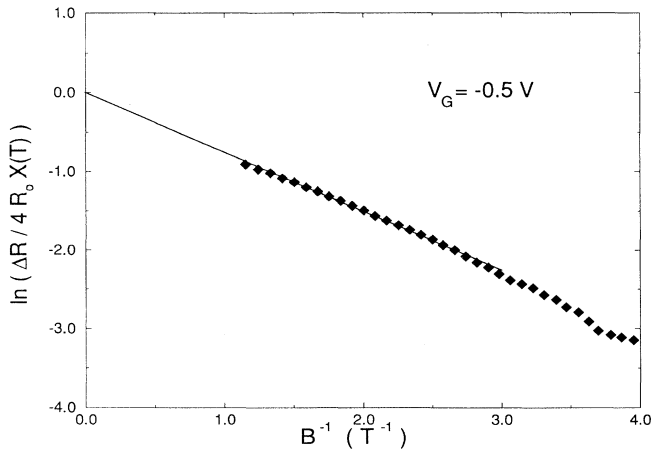


FIG. 4. Dingle plot at a back-gated voltage of -0.5 V. The intercept passes through the origin, which is expected for a good Dingle plot as described in the text.

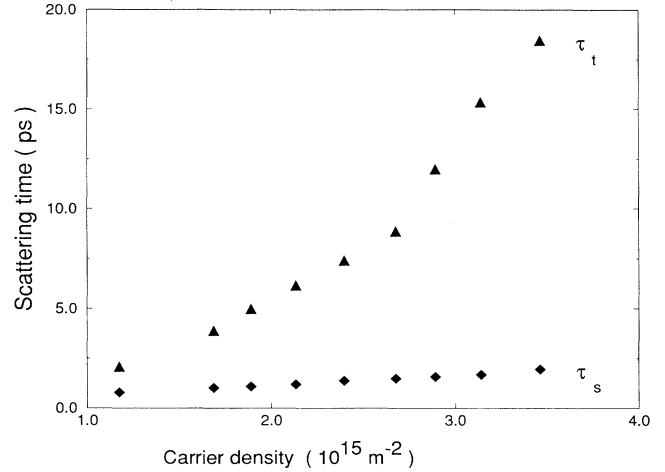


FIG. 5. The transport scattering time and the single-particle scattering time as a function of the carrier density.

the SdH oscillations is given by

$$\Delta R = 4R_0 X(T) \exp(-\pi/\omega_c \tau_s), \quad (3)$$

where R_0 is the zero-field resistance, ω_c is the cyclotron frequency, and $X(T)$ a thermal damping factor, given by

$$X(T) = (2\pi^2 kT / \hbar \omega_c) / \sinh(2\pi^2 kT / \hbar \omega_c). \quad (4)$$

In a Dingle plot, the logarithm of $\Delta R / 4R_0 X(T)$ is plotted against $1/B$, which is a straight line with an intercept of zero. The consequence of nonlinearity in such plots in the low-field region has been discussed at length in Ref. 3. A good Dingle plot is one which is linear and has an intercept of zero. The slope of this straight line gives $1/\tau_s$. The Dingle plots we obtained not only show good linearity, but also have the required intercept.

A typical Dingle plot obtained for our device is shown in Fig. 4. Single-particle scattering times were obtained from Dingle plots at different back-gate voltages. Figure 5 shows the variation of the measured values of τ_t and τ_s with the 2DEG carrier density. It may be noted that τ_t increases more rapidly with increasing carrier density than τ_s .

III. COMPARISON WITH THEORY

Figure 6 shows the ratio τ_t/τ_s as a function of k_F , where $k_F = \sqrt{2\pi n_s}$. It can be seen that the ratio increases with k_F , which is in qualitative agreement with theoretical predictions. The dashed line in Fig. 6 is a plot of the analytical expression given by Gold,² $\tau_t/\tau_s = (2k_F \alpha)^2$, with $\alpha = 200$ Å. The numbers predicted by the theory are too large (by about a factor of 4) compared to the experimental data. Comparison of the experimental data with the theoretical calculations of Das Sarma and Stern¹ also shows large discrepancies between the theoretical and experimental values. In Ref. 3, Coleridge observed a similar discrepancy between the experimental data and theoretical predictions. As described in Ref. 3, the large theoretical estimates of τ_t/τ_s

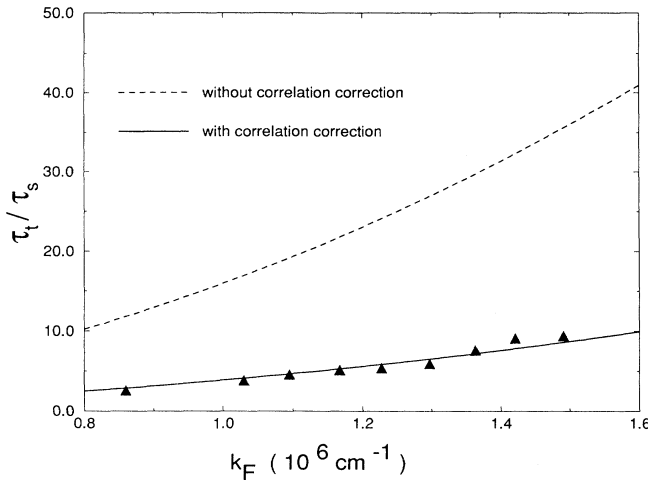


FIG. 6. The ratio of τ_t/τ_s is plotted as a function of k_F . Also shown are the theoretical curves for $\tau_t/\tau_s=(2k_F\alpha)^2$ without (dashed line) and with (solid line) the correlation correction determined in Ref. 3.

arise from neglecting the statistical correlation between multiple small-angle-scattering events. In a modulation-doped heterostructure, the confining potential is the average potential created by the donors. Small-angle scattering is due to the fluctuations in this average potential, and multiple small-angle-scattering events are correlated. Coleridge has used a correlation correction accounting for the interference between the multiple small-angle-scattering events and obtained good match with his experimental data.

The solid line in Fig. 6 is a theoretical plot of the expression $\tau_t/\tau_s=(2k_F\alpha)^2$ with a correlation correction included. The correlation correction was obtained from a comparison of our sample (with no back-gate voltage) with sample no. 350 in Ref. 3, which is quite similar in structure (sample no. 350: $\alpha=205 \text{ \AA}$, $n_s=3.4 \times 10^{15}/\text{m}^2$,

$\tau_t/\tau_s=9.8$, and $\mu_t=45 \text{ m}^2/\text{Vs}$; our sample: $\alpha=200 \text{ \AA}$, $n_s=3.5 \times 10^{15}/\text{m}^2$, $\tau_t/\tau_s=9.43$, and $\mu_t=45 \text{ m}^2/\text{Vs}$). For sample no. 350 in Ref. 3, the calculated values for τ_t/τ_s with and without correlation are 8 and 33, which differ by a factor of 4.1. We assume this value to be the correlation correction factor in our sample. We also assume that the correlation correction factor in our sample does not change significantly with n_s . This assumption is justified since the impurity distribution is not disturbed when the carrier density is varied by the application of a back-gate voltage. It is seen from Fig. 6 that the experimental data match very well with the correlation-corrected theoretical plot.

IV. CONCLUSIONS

In summary, we have examined the variation of the ratio τ_t/τ_s in a two-dimensional electron gas, with carrier concentration. Measurements were performed on a single sample where the carrier density was varied using a back-gate voltage; the spacer layer thickness and the number of ionized donors were unaffected. The background impurity concentration, which is known to affect the scattering times, is also constant since we use a single sample. Results obtained support other observations that the ratio of τ_t/τ_s is enhanced when the scattering is mostly due to long-range scattering potentials. Additionally, the ratio becomes larger with increased carrier density. Comparison of our experimental data with theoretical predictions shows good agreement with the simple model of quadratic dependence on k_F if a correlation correction is assumed.

ACKNOWLEDGMENTS

The authors would like to thank S. Datta for helpful discussions. Work at the University of Notre Dame was supported by the Air Force Office of Scientific Research under Grant No. AFOSR 91-0211 and by the Jesse H. Jones Foundation.

*Present address: ITT Gallium Arsenide Technology Center, Roanoke, VA 24019.

¹S. Das Sarma and F. Stern, Phys. Rev. B **32**, 8442 (1985).

²A. Gold, Phys. Rev. B **38**, 10798 (1988).

³P. T. Coleridge, Phys. Rev. B **44**, 3793 (1991).

⁴B. K. Ridley, Semicond. Sci. Technol. **3**, 111 (1988).

⁵R. Lassnig, Solid State Commun. **65**, 765 (1988).

⁶P. J. van Hall, Superlatt. Microstruct. **6**, 213 (1989).

⁷F. F. Fang, T. P. Smith III, and S. L. Wright, Surf. Sci. **196**, 310 (1988).

⁸U. Bockelmann, G. Abstreiter, G. Weimann, and W. Schlapp,

Phys. Rev. B **41**, 7864 (1990).

⁹J. P. Harrang, R. J. Higgins, R. K. Goodall, P. R. Jay, M. Laviron, and P. Delescluse, Phys. Rev. B **32**, 8126 (1985).

¹⁰R. G. Mani and J. R. Anderson, Phys. Rev. B **37**, 4299 (1988).

¹¹B. Das, S. Subramaniam, and M. R. Melloch (unpublished).

¹²K. Hirakawa and H. Sakaki, Phys. Rev. B **33**, 8291 (1986).

¹³T. Ando, J. Phys. Soc. Jpn. **37**, 1233 (1974).

¹⁴A. Isihara and L. Smrčka, J. Phys. C **19**, 6777 (1986).

¹⁵P. T. Coleridge, R. Stoner, and R. Fletcher, Phys. Rev. B **39**, 1120 (1989).